Proceedings of the
Annual Stability Conference
Structural Stability Research Council
Louisville, Kentucky, April 1-4, 2025

Design and collapse simulation strength sensitivity of large-scale cylindrical tubes for wind turbine support towers in flexure

Xi Peng[1], Dehui Lin[2], Sandor Adany[3], Andrew T. Myers[4], Benjamin W. Schafer[5]

Abstract

The objective of this paper is to explore the predicted strength of large-scale cylindrical tubes manufactured with production methods consistent for wind turbine support towers. A recent series of flexural experimental tests provide benchmarks for the predicted strength. Two numerically-based strength prediction methods motivated by provisions in Eurocode for shell structures are employed herein: (i) direct collapse simulation using geometric and nonlinear shell finite element analysis with imperfections (i.e., GMNIA); and (ii) generalized slenderness predictions that utilize linear buckling analysis (LBA) and material nonlinear analysis (MNA) to form a slenderness parameter and then empirically-derived curves, that are a function of imperfection magnitude, to provide the predicted strength, so-called LBA-MNA methods; including Reference Resistance Design. Sensitivity of the predicted strength to imperfections is of particular interest. The benchmark 1m diameter tubes consisting of varying slenderness, were fabricated using the can-welding process commonly utilized for fabrication of wind turbine support towers and scanned using a high-resolution laser scanner prior to flexural testing. Laser scanning at the weld beads introduces "bumps" in the data that must be removed and then replaced with interpolated data before utilizing the imperfections in GMNIA analysis or characterizing the imperfection magnitudes. A variety of interpolation techniques are explored, detailed, and the implications of the assumptions on predicted strength provided. Strength comparisons are made between GMNIA, LBA-MNA, and the conducted testing – with an emphasis on capturing expected strength sensitivity across the methods. The work is intended to inform a more direct connection between quality of construction (imperfections) and predicted strength and the accurate application of numerical methods in the strength prediction of wind turbine support towers.

1. Introduction

The increasing demand for renewable energy has accelerated the development of larger and more efficient wind turbines to meet global energy needs. These advancements, however, place significant structural demands on support towers, particularly as turbine sizes increase to enhance energy capture. Large-scale thin-walled tubes are commonly employed as wind turbine support

[1] Graduate Research Assistant, Johns Hopkins University, <xpeng26@jhu.edu>
[2] Graduate Research Assistant, Northeastern University, < lin.deh@northeastern.edu>
[3] Associate Research Scientist, Johns Hopkins University, < asandor2@jhu.edu>
[4] Professor, Northeastern University, < an.myers@northeastern.edu >
[5] Professor, Johns Hopkins University, < schafer@jhu.edu >

structures due to their simplicity, manufacturability, and cost-effectiveness. Nonetheless, their mechanical behavior, especially under flexural loading conditions, remains a critical factor in determining their overall performance and reliability. In addition, geometric imperfections are introduced into these large-scale thin-walled cylindrical tubes because of manufacturing processes, where the geometric imperfections may reduce the strength of the tubes by some extent. Therefore, prediction of bending strength of geometrically imperfect cylindrical shells is important during the design process.

Many studies examining the flexural strength of thin-walled steel cylindrical shells have been completed, including analytical solutions, experiments, and numerical simulations. Sadowski, Fajuyitan & Wang. (2017) proposed a computational strategy to establish algebraic parameters for the Reference Resistance Design of metal shell structures, which uses nonlinear finite element simulation results as its original database for RRD parameters calculation. The newest version of Eurocode for shells (CEN 2021) has provided formulae to determine the buckling resistance of unstiffened shells when using Reference Resistance Design (RRD) based on a paper written by Sadowski, Fajuyitan & Wang. (2017). Al-Qureshi (1999) and Karamanos (2002) developed analytical models to quantify the bending (buckling) strength of tubes, where Al-Qureshi (1999) compared results with numerical simulations, and Karamanos (2002) compared results with experimental data. The analytical results showed consistency with numerical simulations and experiments for the slenderness regimes investigated. Various studies have been conducted on bending of thin-walled cylinders over the past decades through experiments. Jay et al. (2016) conducted large scale tests of tapered spirally welded steel tubes (Diameters between 0.7 and 1.1m, and D/t between 200 and 350) and compared test results with design strength per Eurocode for shells (CEN 2021). The collapse load of all specimens exceeded predicted strengths, and all specimens met Eurocode manufacturing quality requirements. Mahmoud et al. (2018) conducted collapse simulation on spiral-welded tubes tested by Jay et al (2016) and proposed basic modeling protocols for GMNIA analysis of thin-walled tubes with imperfections under flexure. Total number of nine flexural tests (as part of a larger series on flexural plus torsion) on 1:4 scale can-welded, thin-walled steel tubes with varying D/t were conducted by Lin et al. (2024). Geometric imperfections of each tube were measured using a high-resolution laser scanner. A common trend that all three specimens was an initial linear response followed by a sudden decrease in moment due to buckling, but the nonlinearity and post-buckling behavior varied for each tube, suggesting sensitivity in the response. Peng et al. (2024) has performed GMNIA analysis for can-welded tube tested by Lin et al. (2024) using both idealized imperfections and scanned imperfections with both ABAQUS and ANSYS, where the simulated results using both idealized imperfections and scanned imperfections agrees well with the test data, and results from ABAQUS and ANSYS show consistency.

The objective of this study is to further investigate modeling protocols for analyzing flexural collapse of thin-walled cylindrical shells, which are usually employed as the supporting structure of wind turbines, by conducting GMNIA analysis using measured imperfections. The modeling protocols include specifying material properties for each can in a given test specimen, considering small strain effects for each can, and taking care with interpolation of the imperfection data around "weld beads". Interpolation across the weld bead location using different mathematical forms are considered. Numerical results of the different interpolation methods are compared with the three benchmark test results from Lin et al. (2024). In the end, simulated strength of the different

interpolation methods are compared with strength calculated from Reference Resistance Design (RRD) as detailed in Eurocode (CEN 2021).

2. Test summary

Three benchmark tests on the flexural strength of 1:4 scale can-welded thin-walled cylindrical shells with different D/t ratios have been conducted in the STRess Lab in Northeastern university (Lin et al 2024). The geometry of the nominal can-welded tube can be defined by three parameters: diameter (D), thickness (t), and length (L) as summarized for the nine tested specimens in Table 1. The length and diameter of the three specimens is the same (D = 1003 mm, L = 3302 mm), and their thickness is different, which varies the D/t ratio from 158 to 315.

Table 1: Summary of geometry of specimens

Specimens	D(mm)	t(mm)	L(mm)	D/t
CW-158-1	1003	6.35	3302	158
CW-211-3	1003	4.76	3302	211
CW-315-3	1003	3.175	3302	315

A picture of the test rig and schematic diagram (Lin et al 2024) is shown in Fig. 1. The specimen is fabricated from five small cans: L1, L2, M, R2, and R1 as indicated. The specimen is welded to thick endplates at its two ends, and the two endplates are connected to stiff crossbeams. Pure bending is applied to the specimen by rotation of both ends of the specimen through two hydraulic actuators (one hydraulic actuator applies compression in displacement control, and the others applies tension in force control). As shown in Fig. 1, the upper part of the tube is the tension side, and the lower part of the tube is the compression side. The left end of the specimen is a pin end, which constrains longitudinal, transverse and torsional displacement. The right end of the specimen is a slot end, which releases the longitudinal displacement. The test procedure is as follows: (1) the specimen is scanned by a high-resolution laser scanner to obtain the magnitude and distribution of initial geometric imperfections in the tube; (2) a small amplitude load cycle is applied to the specimen to estimate frictional moment between the tube and the test rig; (3) as the loading begins, the test is regularly paused for laser-scanning the compression zone of the specimen; (4) the test is complete when the total rotation of the two ends of the specimen reaches 2 degrees, or fracture occurs.

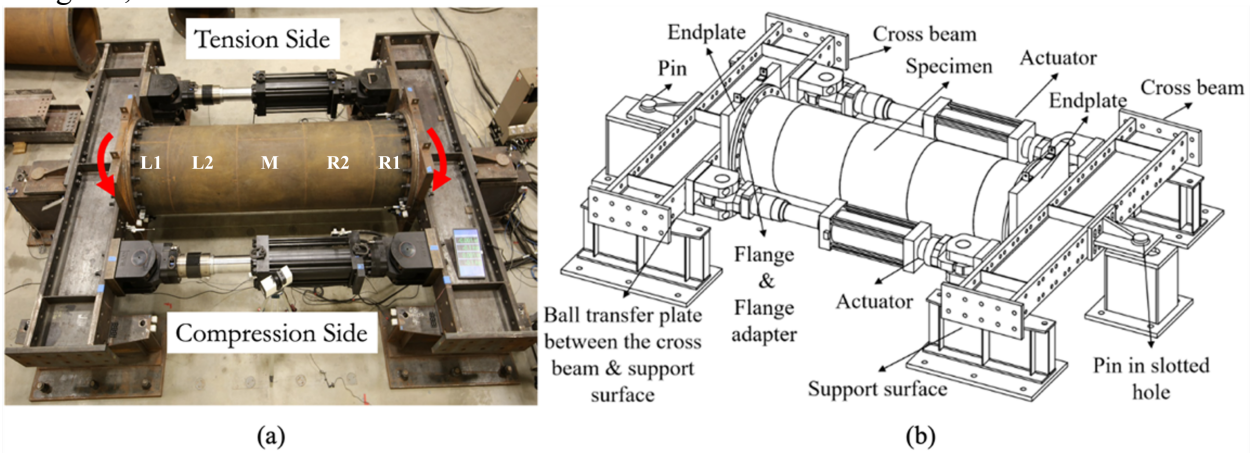

Figure 1: (a) Picture of test rig; (b) Schematic diagram of test rig (Lin et al 2024)

3. Modeling protocols

3.1 Mesh and Boundary conditions

All of the GMNIA analyses are performed in the commercial finite element software ABAQUS with the input files being produced through a custom MATLAB script. Mesh size of each specimen is set to $0.25\sqrt{Rt}$ with a 1:1 aspect ratio, as recommended by Mahmoud (2017). As a result, the mesh size for tubes with D/t = 158, 211, and 315 are 14mm, 12mm, and 10mm, respectively. The finite element mesh and coordinate system is shown in Fig. 2, where the mesh size of each plot is different. The element type used in ABAQUS simulation is S4R. Reference points at the two ends (RP1 and RP2) of the finite element models are coupled with nodes at the corresponding end by MPC beam constraints. For displacement boundary conditions, the longitudinal, transverse and torsional displacement of the point RP1 (pin end) is constrained, and RP2 is similar but with the longitudinal displacement released (slot end). The color in Fig. 3 represents different material properties, and the name of each section from right (green) to left (grey) is L1, L2, M, R2, R1.

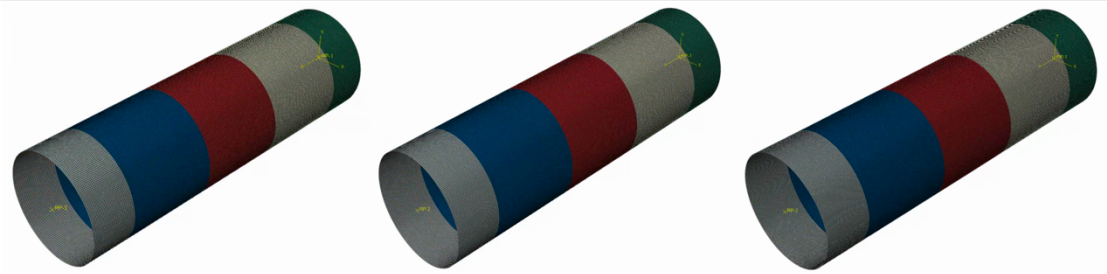

Figure 2: (a) FEM mesh for specimen with D/t = 158; (b) FEM mesh for specimen with D/t = 211; (c) FEM mesh for specimen with D/t = 315

3.2 Material properties

The engineering yield stress (f_y) of each can of each tube is provided in Table 2, and coupon test results of each can of each specimen are shown in Fig. 3(a). The engineering yield stress (f_y) is the determined using the 0.2% offset method. The yield stress and stress – strain relations are nearly the same for each can of each specimen, with only the ultimate strain exhibiting consistent differences. Qualitatively the steel for D/t=315 has a classical sharp yielding nature, while the other two steels exihibit more gradual yielding; with the D/t=211 tube having substantial strain hardening and the D/t=158 tube having minimal strain hardening. As shown in Fig. 3(a), the real behavior of material of CW-158-1 and CW-211-3 is not linear up to f_y. To capture the material response in the simulation, the end of the elastic regime and start of the plastic stress – plastic strain relations are all set to $0.6f_y$. Peng et al. (2024) has compared GMNIA results between models using $1.0f_y$ proportional limit and that using $0.6f_y$ proportional limit. The results show that GMNIA models using $1.0f_y$ proportional limit are not able to capture the softening before yielding and the buckling type is changed in some cases with $1.0\ f_y$ proportional limit, which may provide great error in stiffness predictions. The illustration of this proportional limit choice for the tube material is shown in Fig. 3(b). The engineering stress and strain are converted into true stress and strain, and then inputted into the FEM solver.

Table 2: Summary of engineering yield stress (f_y) of each can of tube (Unit: MPa)

Specimen	L1	L2	M	R2	R1
CW-158-1	408.97	404.92	410.24	412.93	412.93
CW-211-3	454.56	438.91	451.55	452.85	440.94
CW-315-3	417.07	420.96	419.71	408.21	415.01

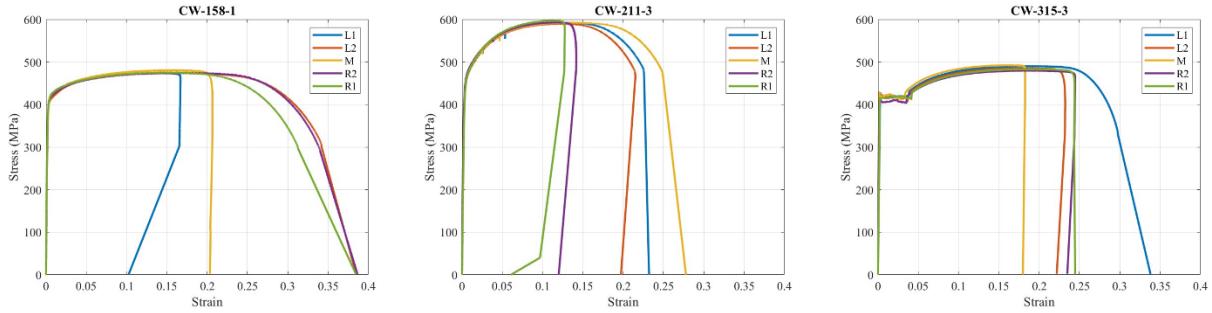

Figure 3: (a) Coupon test results of each specimen

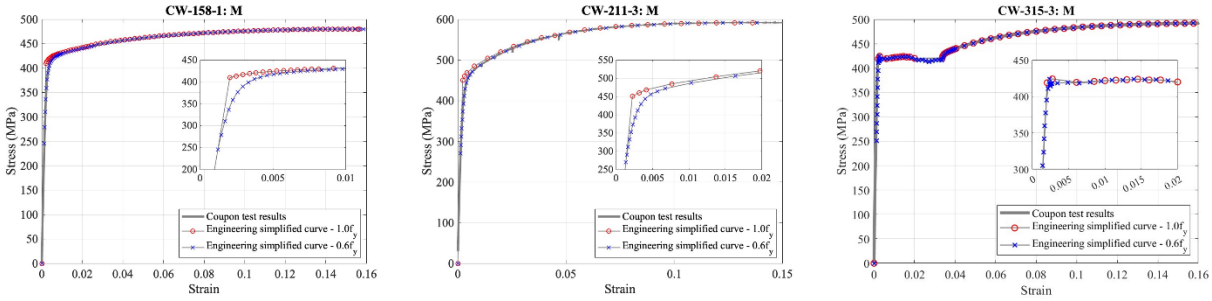

Figure 3: (b) Illustration of proportional limit of tube material

3.3 Interpolations of scanned imperfections

The magnitude of radial geometric imperfections are obtained using a high-resolution laser scanner with 1mm resolution, and the original scanned imperfections of all specimens are shown in Fig. 4. However, radial imperfections around the weld region are not known due to existence of weld bead, which appears as a small discontinuity on the imperfection field (see the dark line in Fig. 4). To tackle this issue, the imperfection values around the weld bead are interpolated using different methods: Fourier series (FS), Linear interpolation (L), 4th order polynomial (4th), Linear interpolation for circumferential welds plus Fourier series for seam welds (L + FS), and 4th order polynomial for circumferential welds plus Fourier series for seam welds (4th + FS).

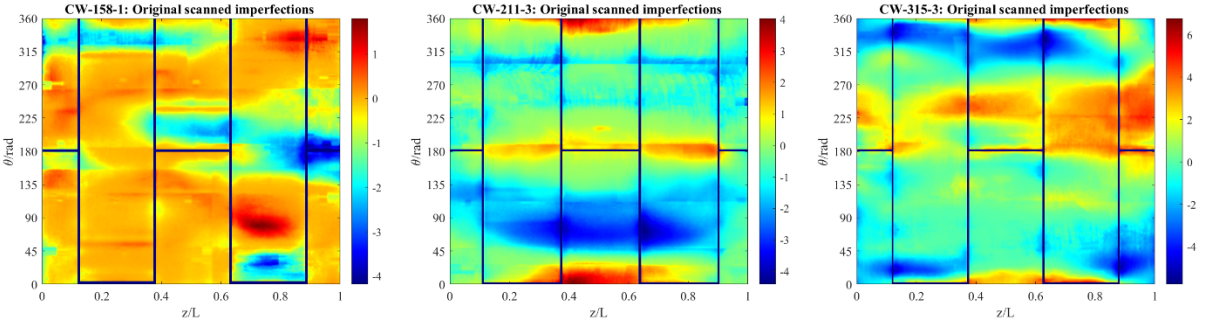

Figure 4: Original scanned imperfections

The procedure of obtaining the Fourier series approximation of the imperfection magnitude is provided in Peng et al. (2024). For linear interpolations and 4th order polynomial fitting, a straight line or a curve with 4th order polynomial form is best fit and used for approximating the imperfections at the weld bead region. The interpolated scanned imperfections are shown in Fig. 5 ~ 7. The interpolated region generally agrees well with its surroundings. Imperfection details at the interpolated region for Fourier series, linear interpolation, and 4th order polynomial are provided in Fig. 8. Linear interpolation simply connects two curves with a straight line, whereas the fourth-order polynomial produces the smoothest fit. By contrast, the imperfections derived from the Fourier series exhibit a small jump at both the left and right boundaries of the weld bead, because limited terms of the Fourier series are considered. If more Fourier terms are considered, the jump could be eliminated. The expected form for a weld depression imperfection is well approximated by a 4th order polynomial.

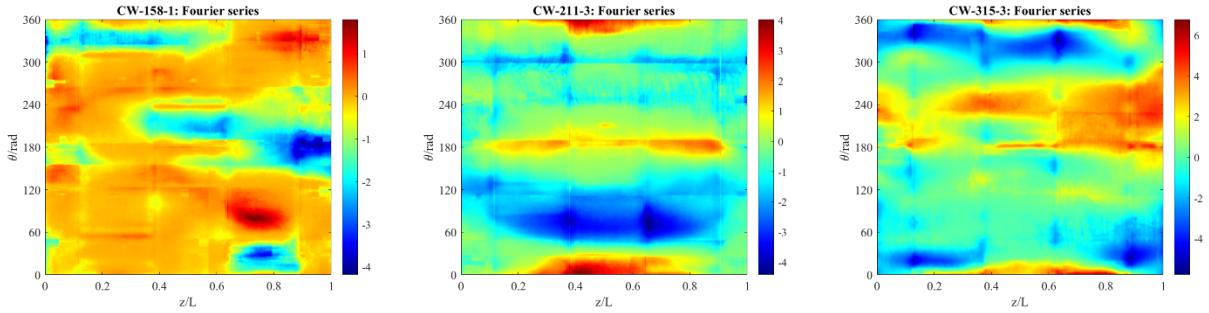

Figure 5: Interpolated imperfections using Fourier series for both seam welds and circumferential welds

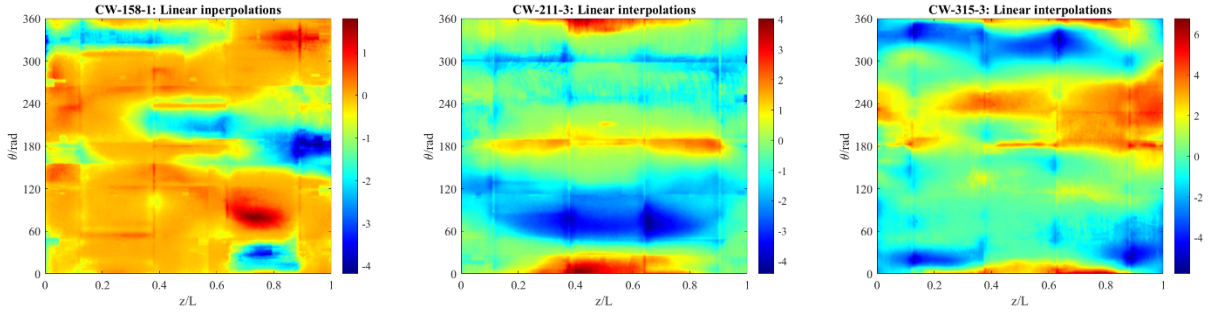

Figure 6(a): Interpolated imperfections using Linear interpolation for both seam welds and circumferential welds

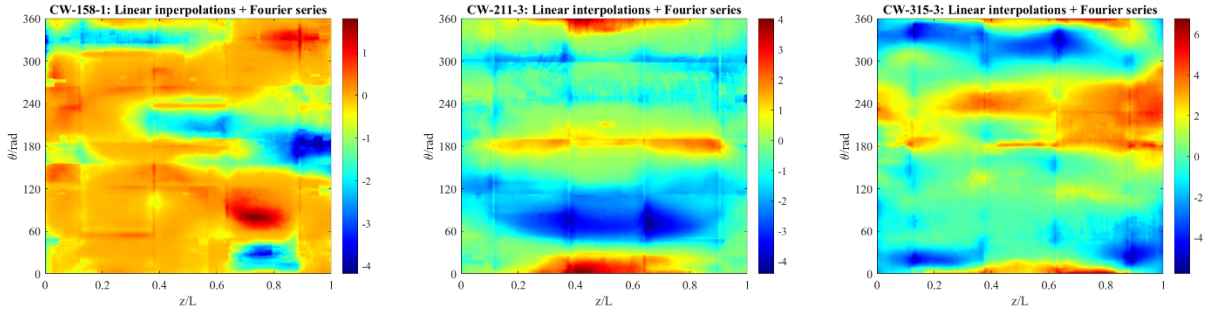

Figure 6(b): Interpolated imperfections using Linear interpolation for circumferential welds and Fourier series for seam welds

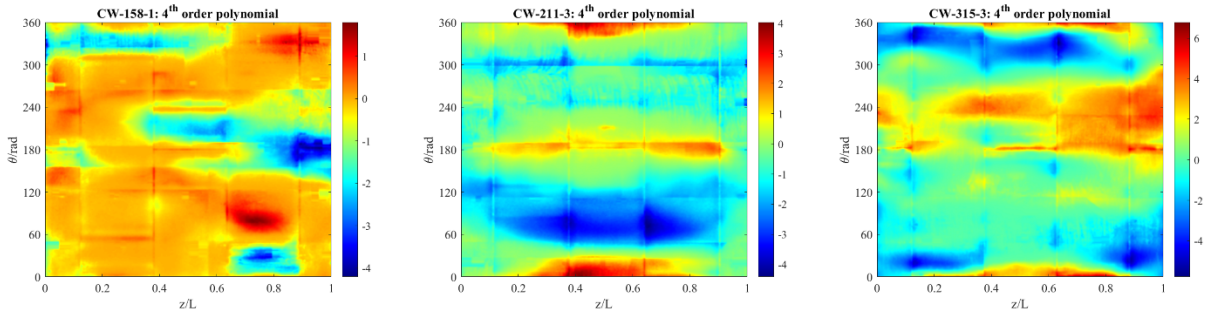

Figure 7(a): Interpolated imperfections using 4th order polynomial for both seam welds and circumferential welds

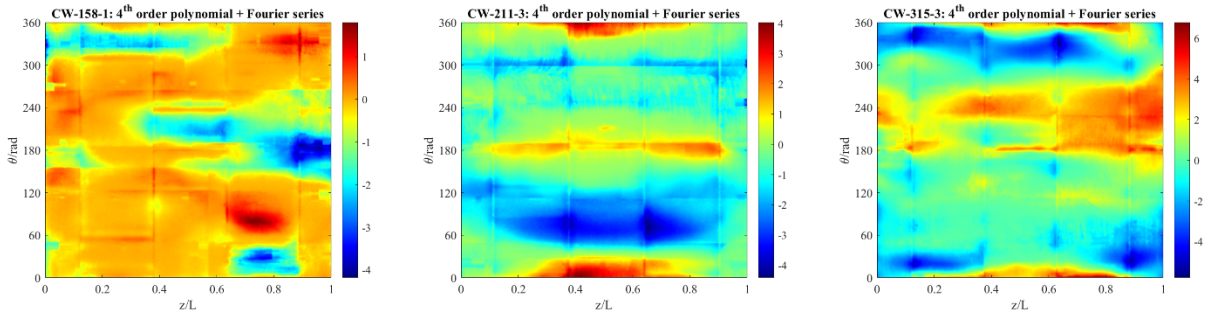

Figure 7(b): Interpolated imperfections using 4th order polynomial for circumferential welds and Fourier series for seam welds

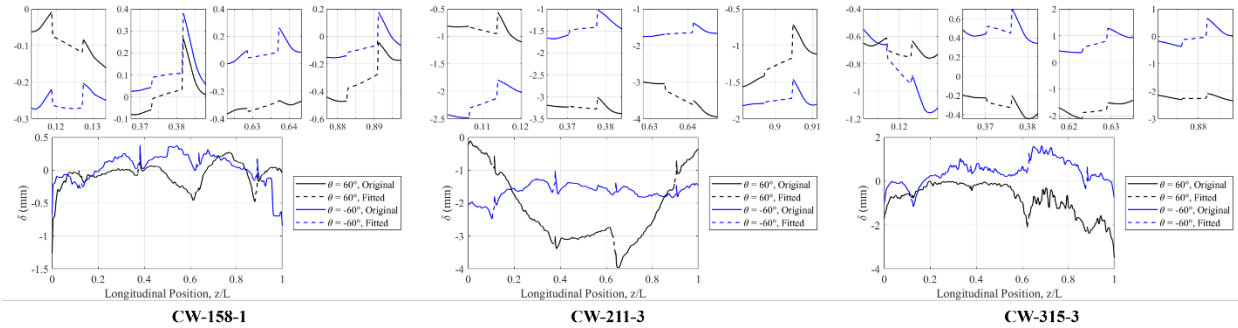

Figure 8(a): Details of scanned imperfections using Fourier series

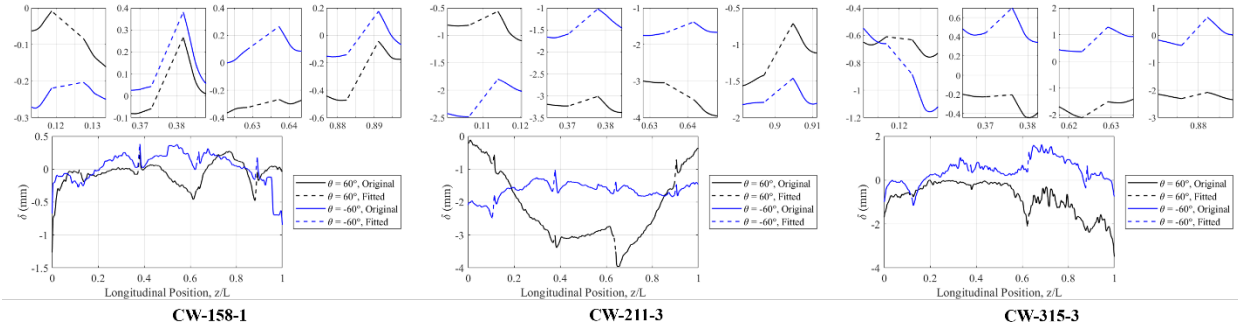

Figure 8(b): Details of scanned imperfections using linear interpolation

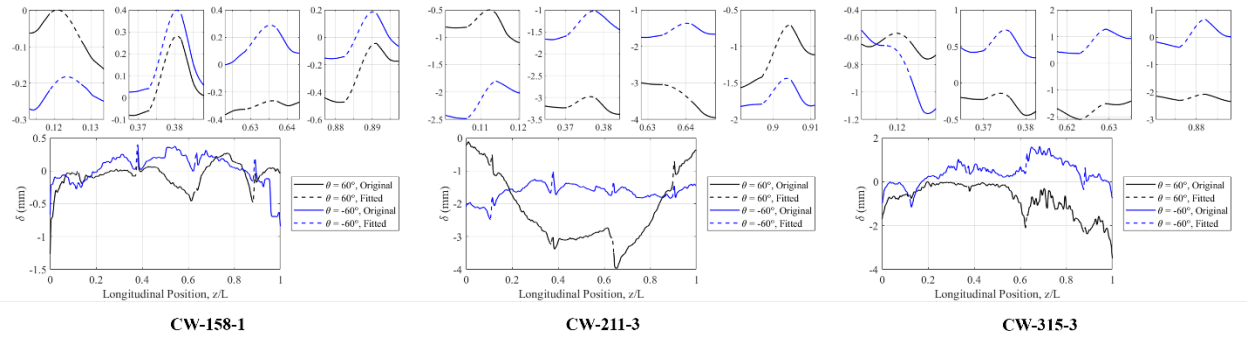

Figure 8(c): Details of scanned imperfections using 4th order polynomial fitting

4. GMNIA results

Comparison between peak load from the GMNIA and test are provided in Table 3. The peak load from GMNIA using the different interpolation methods is nearly the same, indicating that the interpolation of the imperfections at the weld bead has only a mild influence on the strength of the specimens (this is somewhat surprising since previous research has highlighted that imperfections at the weld locations are the most influential for predicting flexural strength (Wang et al. (2020))). In comparison with the tested strength of the specimens, the simulated strength of CW-158-1 is 11% higher than the tested one, where the simulated strength of CW-315-3 is 4% lower than the tested one. For specimen CW-211-3, its simulated strength agrees well with the test.

Table 3: Comparison between peak load of GMNIA and test

Specimen	Imperfections type	M_{test} (kN · m)	M_{GMNIA} (kN · m)	M_{GMNIA}/M_{test}
CW-158-1	FS	1994	2264	1.14
	L		2261	1.13
	L + FS		2261	1.13
	4th		2242	1.12
	4th + FS		2242	1.12
CW-211-3	FS	1522	1562	1.03
	L		1561	1.03
	L + FS		1561	1.03
	4th		1557	1.02
	4th + FS		1557	1.02
CW-315-3	FS	918	872	0.95
	L		883	0.96
	L + FS		883	0.96
	4th		882	0.96
	4th + FS		882	0.96

Fig. 9 shows comparison of the moment-rotation curve and post-buckling behavior between GMNIA and the tests. Following the moment-rotation curve, (material) nonlinear behavior is exhibited in the pre-peak region of the first two specimens, while the thinnest specimen

experiences elastic buckling. After the first bifurcation point, the evolution of moment with the total rotation follows almost the same path, with a slight difference in the simulated strength. Notably, the simulated stiffness of the first (thicker) specimen is higher than that of the test above ~ 1000 kN-m. As the D/t ratio increases (and moment decreases), the stiffness of the specimens in numerical simulations agrees better with the test. For the post-buckling behavior, the thinnest tube has the same post-buckling behavior in numerical simulations as the test. However, the post-buckling behavior of the first two specimens in the numerical simulations has some differences relative to the corresponding test. Specimen CW-158-1 buckled at the end plate during test, but buckled at the middle of the tube in the numerical simulation. Specimen CW-211-3 buckled in the test close to its second weld (from the left to the right), while the buckling location in the numerical simulation is near the third circumferential weld.

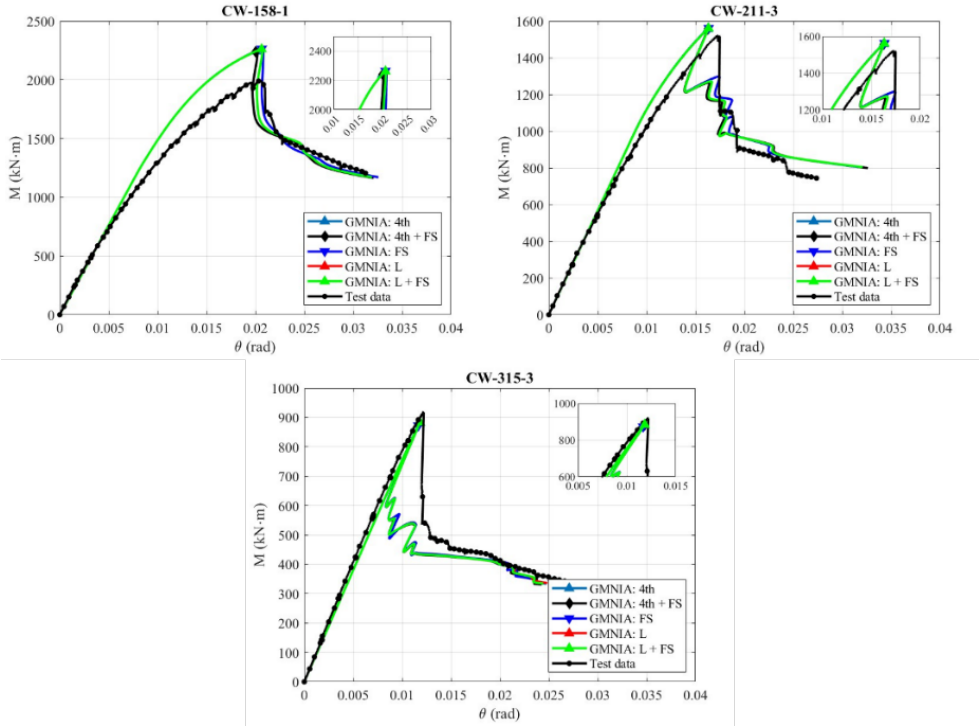

Figure 9 (a). Comparison of Moment – rotation curve between GMNIA with different imperfections interpolation methods and test

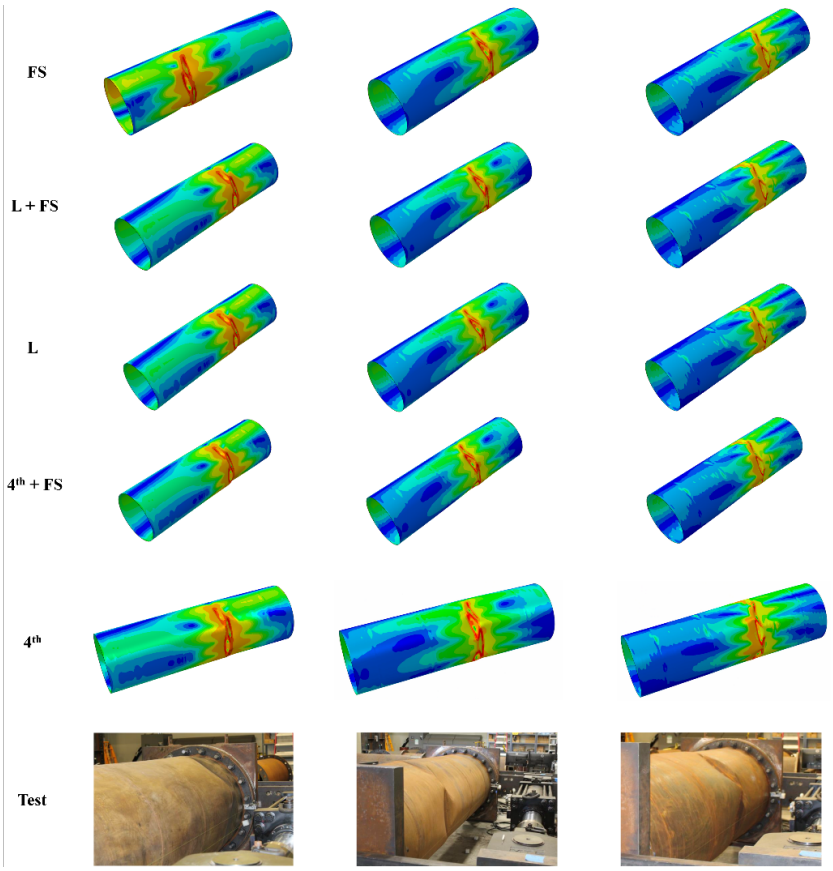

Figure 9 (b). Comparison of Post-buckling behavior between GMNIA with different imperfections interpolation methods and test

Comparison between the normalized peak load of GMNIA and normalized strength calculated using Reference Resistance Design (RRD) are provided in Fig. 10. Strength of each specimen is normalized by its plastic moment ($M_p = 4\pi r^2 t f_y$). The numerical solutions for the specimen capacity obtained using different interpolation methods are all higher than the Class A strength determined by the RRD, so the codified design method appears to provide conservative results in this study. In addition, the tested capacity has larger difference with that calculated from RRD as the D/t ratio becomes larger. In the RRD model developed by Sadowski, Fajuyitan & Wang. (2017), the material models for their nonlinear finite element models are typically elastic – perfectly plastic to align with Eurocode material assumptions, and this may contribute to the reason why the tested capacity has larger difference with that calculated from RRD, although the difference in the most slender tube should not be influenced significantly by this assumption so further investigation is needed.

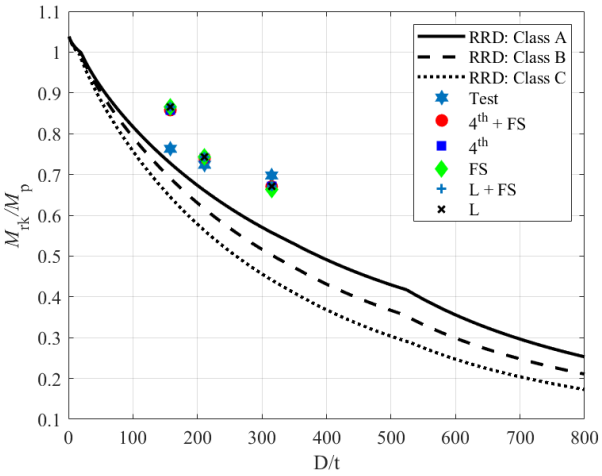

Figure 10. Comparison of design method

5. Discussion

The relatively favorable agreement between the numerical models and the tests in this study shows the effectiveness of the proposed modeling protocols for collapse analysis of thin-walled steel cylinder with measured imperfections. In total five interpolation methods are used to obtain reasonable values of geometric imperfections at the weld bead region. Only slight differences are exhibited in the moment-rotation curve and simulated strength of the specimen under these different interpolation methods. Also, by comparing the simulated strength with the strength calculated from RRD, we can see that strength calculated from RRD against these tests appears conservative. However, the GMNIA simulated bending strength of the first specimen CW-158-1 is almost 12% higher than the tested bending strength, this is possibly due to insufficient weld penetration in the specimens, which reduces its strength. Also, the response of the specimen CW-158-1 and CW-211-3 in the GMNIA numerical simulation is stiffer than that in test above a certain level of moment (initial stiffness is accurate, but the tested stiffness decreases pre-peak faster than the GMINA simulation). One possible cause for this reduction in stiffness is yielding within the welds where full penetration was not achieved, but further work is needed to validate this hypothesis.

6. Conclusions

A shell finite element-based modeling protocol for collapse simulation of large cylindrical steel tubes in flexure, consistent with manufacturing and slenderness utilized in wind turbine support towers is developed. Three recent flexural tests on 1m diameter tubes that had detailed laser scanning of initial geometric imperfections conducted prior to testing are employed for validation. The geometric and material nonlinear analysis with imperfections (GMNIA) collapse simulation must faithfully reproduce the material and geometric imperfections in the testing to provide an accurate result. This requires detailed knowledge of the stress-strain relationships, which in the case of the testing varied can-by-can along the length in some cases. This also required detailed knowledge of the imperfections, which are available through scanning but require processing and some interpolation to provide a full-field measurement. GMNIA simulations agree well with the testing, particularly with respect to strength – and the most slender tubes exhibit the best overall agreement in response. Pre-peak stiffness in the stockier tubes is experimentally lower than predicted in the models and additional investigation is needed to resolve this discrepancy. In

comparison with Eurocode's implementation of Reference Resistance Design (RRD), which is itself based on GMNIA modeling, the results indicate that the current tests and GMNIA simulations predict higher capacities than RRD, suggesting further refinements may be possible.

Acknowledgments

The authors would like to acknowledge Victoria Ding, Ziqi Tang, Saravanan Subramanian, Anil Pervizaj, and Søren Bøgelund Madsen who contributed to discussions on this work. This paper is based upon work supported by the National Science Foundation under grants CMMI-1334489 and CMMI-1334122. Any opinions, findings, and conclusions or recommendations expressed in this material are those of the author(s) and do not necessarily reflect the views of the National Science Foundation.

References

CEN (European Committee for Standardization). (2021). "Design of steel structures. Part 1-6: Strength and stability of shell structures." *EN 1993-1-6, Eurocode 3*, Brussels, Belgium.

Karamanos, S. A. (2002). Bending instabilities of elastic tubes. *International Journal of Solids and Structures*, *39*(8), 2059-2085.

Al-Qureshi, H. A. (1999). Elastic-plastic analysis of tube bending. *International Journal of Machine Tools and Manufacture*, *39*(1), 87-104.

Peng, X., Lin, D., Saravanan, S., Pervizaj, A., Myers, A., Schafer, B. (2024) Collapse modeling of thin-walled cylinder with measured imperfections. Structural Stability Research Council Annual Stability Conference, March 2024, San Antonio, TX

Mahmoud, A., Torabian, S., Jay, A., Mirzaie, F., Myers, A. T., Smith, E., & Schafer, B. W. (2018). Modeling the flexural collapse of thin-walled spirally welded tapered tubes. *Journal of Structural Engineering*, *144*(2), 04017201.

Jay, A., Myers, A. T., Mirzaie, F., Mahmoud, A., Torabian, S., Smith, E., & Schafer, B. W. (2016a). Large-scale bending tests of slender tapered spirally welded steel tubes. *Journal of Structural Engineering*, *142*(12), 04016136.

Lin, D., Pervizaj, A., Madsen, S.B., Myers, A. (2024) "Flexural buckling tests on 1:4 scale wind turbine tower tubes." Structural Stability Research Council Annual Stability Conference, March 2024, San Antonio, TX

Mahmoud, A. (2017). Analysis and Design of Spirally Welded Thin-Walled Steel Tapered Cylindrical Shells Under Bending with Application to Wind Turbine Towers (Doctoral dissertation, Johns Hopkins University).

Sadowski, A. J., Fajuyitan, O. K., & Wang, J. (2017). A computational strategy to establish algebraic parameters for the Reference Resistance Design of metal shell structures. *Advances in Engineering Software*, *109*, 15-30.

Wang, J., Fajuyitan, O. K., Orabi, M. A., Rotter, J. M., & Sadowski, A. J. (2020). "Cylindrical shells under uniform bending in the framework of Reference Resistance Design." *Journal of Constructional Steel Research*, 166, 105920.